Magnetic Resonance Imaging Indicates Decreased Choroidal and Retinal Blood Flow in the DBA/2J Mouse Model of Glaucoma

William J. Lavery, Eric R. Muir, Jeffrey W. Kiel, and Timothy Q. Duong

Purpose. This study tests the hypothesis that reduced retinal and choroidal blood flow (BF) occur in the DBA/2J mouse model of glaucoma.

Methods. Quantitative BF magnetic resonance imaging (MRI) with a resolution of 42 × 42 × 400 μm was performed on DBA/2J mice at 4, 6, and 9 months of age and C57BL/6 age-matched controls under isoflurane anesthesia. BF MRI images were acquired with echo-planar imaging using an arterial spin labeling technique and a custom-made eye coil at 7 Tesla. Automated profile analysis was performed to average layer-specific BF along the length of the retina and choroid. In separate experiments, servo-null micropressure measurements of iliac arterial pressure were performed in old mice of both strains.

Results. Choroidal BF was lower in DBA/2J mice than in age-matched C57BL/6 control mice at 4, 6, and 9 months of age ($P < 0.01$ for all age-matched groups). Retinal BF was lower in DBA/2J mice than in C57BL/6 mice at the 9-month time point ($P < 0.01$). Mean arterial pressure was not significantly different in aged C57BL/6 mice compared with aged DBA/2J mice.

Conclusions. The reduced ocular blood flow in DBA/2J mice compared with C57BL/6 control mice suggests that ischemia or hypoxia should be considered as a possible contributing factor in the optic neuropathy in the DBA/2J mouse model of glaucoma. (*Invest Ophthalmol Vis Sci.* 2012;53:560–564) DOI: 10.1167/iovs.11-8429

Animal models of glaucoma often use ocular hypertension as the foundation for studying anatomic changes, physiological regulation, and disease mechanisms.[1,2] One widely used model is the DBA/2J mouse.[3–5] This mouse has mutations that cause expression of two aberrant proteins: tyrosinase-related protein 1 (Tyrp1), which causes iris stromal atrophy,[6] and glycoprotein transmembrane nmb (Gpnmb), thought to cause iris pigmentary dispersion, which increases intraocular pressure (IOP) by obstructing the trabecular meshwork and decreasing trabecular outflow facility.[7] The DBA/2J mouse develops ocular hypertension and optic neuropathy at the age of 4 to 6 months. It is unknown whether the ocular hypertension impairs ocular blood flow (BF) in the DBA/2J mouse and contributes to the optic neuropathy.

MRI allows for the study of anatomy, blood flow, and responses to stimulations (so-called functional MRI) in a noninvasive manner without depth limitation or image aberrations caused by tissue density variations that hinder optical methods. MRI is popular in neuroscience research, particularly to image brain anatomy and functional responses to sensory or cognitive stimuli. In addition, BF can be quantitatively measured with an MRI technique called arterial spin labeling (ASL).[8,9] The resolution of these MRI modalities is sufficient for studying small organs and tissues, including those of the mouse eye.[10] Given this MRI capability and the lack of information about ocular BF in the DBA/2J mouse, this study sought to test the hypothesis that ocular BF is reduced in the DBA/2J mouse over the time course of its development of ocular hypertension and optic neuropathy. Age-matched C57BL/6 mice were used as controls, as in other DBA/2J studies.[11,12]

Methods

The protocols were reviewed and approved by the local Institutional Animal Care and Use Committee in accordance with the Guide for the Care and Use of Laboratory Animals and adhered to the ARVO Statement for the Use of Animals in Ophthalmic and Vision Research.

Animal Preparation

DBA/2J mice (Jackson Laboratories, Bar Harbor, ME) aged 4 months ($n = 10$), 6 months ($n = 5$), and 9 months ($n = 5$) and C57BL/6 mice (Charles River Laboratories, Wilmington, MA) aged 4 months ($n = 5$), 6 months ($n = 8$), and 9 months ($n = 7$) were imaged with MRI. Animals were placed in a holder with ear and tooth bars to minimize motion. During imaging, mice spontaneously breathed a mixture of 30% O_2/70% N_2 with 1.6% isoflurane for anesthesia. The respiratory rate was monitored, and slight adjustments were made to the anesthesia level to keep the respiratory rate in a target range of 80 to 120 breaths/minute. Heart rate, temperature, and O_2 saturation were also monitored. Animal temperature was monitored and maintained at 37°C with warm water that circulated through a water pad on which the mouse laid for the duration of the experiment.

MRI Measurements

Depth-resolved quantitative BF MRI was performed at a resolution of 42 × 42 × 400 μm. MRI scans were performed in a 7 Tesla magnet instrument (Biospec; Bruker, Billerica, MA) with a 150 Gauss/cm gradient using a custom eye coil for imaging (diameter, 6 mm) and a heart coil for ASL (diameter, 8 mm) (Fig. 1). The BF scans were acquired with a gradient-echo, echo-planar imaging sequence with a 6 × 6 mm field of view and 144 × 144 matrix (42 × 42 μm resolution in-plane) zero-filled interpolation to 256 × 256. The BF sequence used a single, 400-μm coronal slice, 2 shots, 2.94-second labeling pulse, 3.0-second repetition time, and 13-ms echo time. The slice was positioned near

From the Department of Ophthalmology and Research Imaging Institute, University of Texas Health Science Center, San Antonio, Texas.

Supported by the San Antonio Life Science Institute; National Institutes of Health Grants EY009702, EY014211, and EY018855; Department of Veterans Affairs MERIT Award; and Clinical Translational Science Award Parent Grant UL1RR025767.

Submitted for publication August 16, 2011; revised November 15, 2011; accepted December 10, 2011.

Disclosure: **W.J. Lavery**, None; **E.R. Muir**, None; **J.W. Kiel**, None; **T.Q. Duong**, None

Corresponding author: Timothy Q. Duong, University of Texas Health Science Center at San Antonio, Research Imaging Institute, 8403 Floyd Curl Drive, San Antonio, TX 78229; duongt@uthscsa.edu.

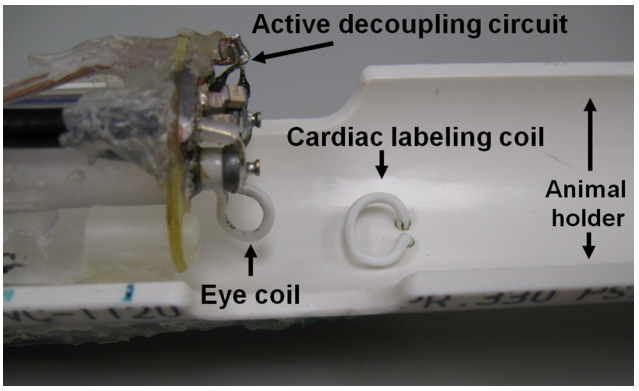

FIGURE 1. Animal holder with imaging coils. Mouse lies at location marked *animal holder*. Labeling pulses are transmitted to mouse's heart through the *cardiac labeling coil*, and ocular BF is imaged by the *eye coil*. An active decoupling circuit is used to prevent interference of the signals sent or received by the cardiac and eye coils.

the optic nerve and tilted to be perpendicular to the retina. BF values were calculated from images acquired over a 20-minute period and were averaged offline.

Arterial Pressure Measurements

To measure arterial pressure, separate groups of C57BL/6 mice ($n = 9$) and DBA/2J ($n = 9$) mice, all aged 6 months and older, were anesthetized with 1.6% isoflurane as described. An iliac artery cutdown was performed. Arterial pressure in the iliac artery was measured for 1 hour using a servo-null micropressure system (model 900A; World Precision Instruments, Sarasota, FL). The technique made use of glass micropipettes drawn to a 3- to 5-μm diameter tip to cannulate a target blood vessel. The pipette was filled with 2 M NaCl that permits an electric circuit to be established between the pipette and a reference electrode placed in the tissue nearby. The resistance across the pipette tip was monitored, and a pressure pod with a fast piezo-electric valve applied the necessary pressure to the open end of the pipette that maintains the resistance constant at the tip in the vessel. The applied pressure was taken to be equivalent to the pressure in the vessel. After the experiment, the mice were euthanized without regaining consciousness.

Statistical Analysis

Data analysis was performed with custom software packages (MatLab [MathWorks Inc, Natick, MA]and STIMULATE [Center for Magnetic Resonance Research, University of Minnesota, www.cmrr.umn.edu/stimulate/non_frame/index.html]) as described in detail elsewhere.[13,14] A semi-automated process in MatLab was used to linearize the retina, align it to correct for motion (if any) of the eye during the scan, and conduct an automated profile analysis.[10] Profiles across the retinal thickness were obtained from images by projecting lines perpendicular to the retina with profiles obtained at 4 $\times$ spatial interpolation. The BF (mL/min/g) was calculated from the signal intensities of labeled and nonlabeled images, as follows[15,16]:

$$BF = (\lambda/T_1)\,(S_{NL} - S_L)/[S_L + (2\alpha - 1)S_{NL}]$$

In this formula, λ (0.9 mL/g)[17] is the tissue-blood partition coefficient for water and is the value [(quantity of water/g tissue)/(quantity of water/mL blood)]. T_1 is 1.8 seconds at 7 Tesla,[18] S_{NL} is the signal intensity (arbitrary units) of images with nonlabeled blood, S_L (arbitrary units) is the signal intensity of images with magnetically labeled blood, and α is the arterial spin-labeling efficiency (0.7)[10] for cardiac labeling in mice. BF profiles were averaged along the length of the retina, as shown in Figure 2. Two peaks were present in the averaged BF profile, located in the inner retina and choroid. Measurements of retinal and choroidal BF were determined from the corresponding peaks from the average BF profiles for each animal.

Data are reported as mean $\pm$ SD, with statistically significant differences reported when $P < 0.05$. One-way ANOVA with Tukey's multiple comparisons test was used to determine differences in choroidal or retinal blood flow within strains. Two-way ANOVA with the Bonferroni posttest was used to determine differences in choroidal or retinal blood flow by age between strains. An unpaired *t*-test was used to compare strain means (Prism; GraphPad, La Jolla, CA).

RESULTS

Representative BF images are shown in Figure 2. Choroidal BF (Fig. 3, left) in C57BL/6 mice was 7.14 $\pm$ 1.4 (range, 4.7–8.3) mL/min/g at 4 months of age, 5.29 $\pm$ 1.4 (range, 2.5–6.8) mL/min/g at 6 months of age, and 5.20 $\pm$ 1.3 (range, 3.1–7.0) mL/min/g at 9 months of age. Although trending downward with age, choroidal BF in the C57BL/6 mice was not significantly

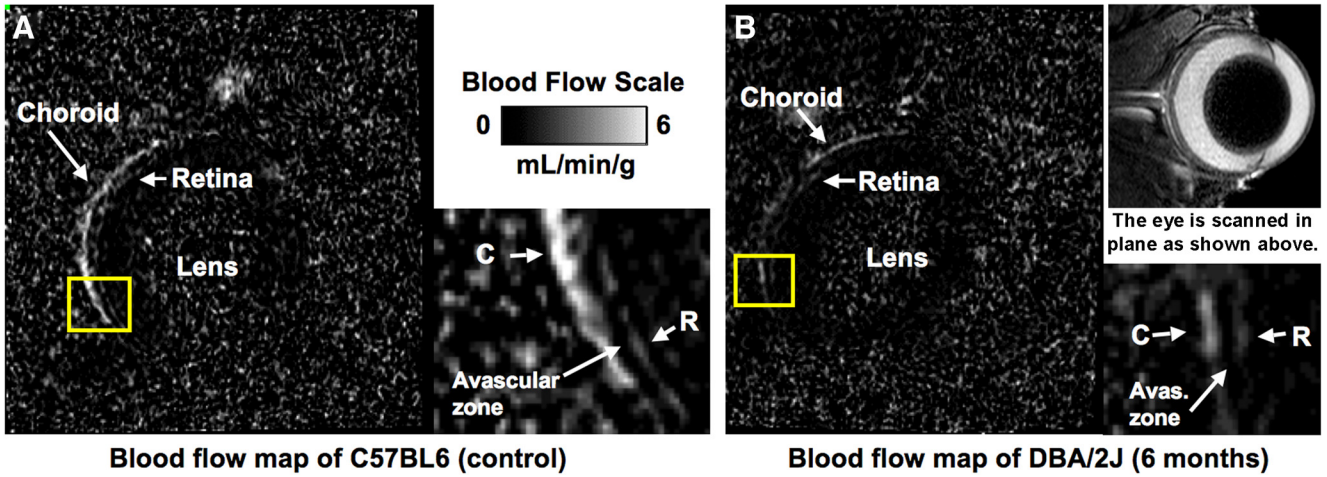

FIGURE 2. Calculated BF maps at a resolution of 42 $\times$ 42 $\times$ 400 μm on a scale of 0 to 6 mL/min/g. (**A**) BF map of a C57BL/6 control mouse. BF maps resolve choroidal and retinal vascular layers with the avascular zone between. (*white arrowheads*) Region of the retina used typically for BF analysis. (**B**) BF map of a 6-month-old DBA/2J mouse, which has lower choroidal and retinal BF. (Anatomic image from another animal shows scan orientation.)

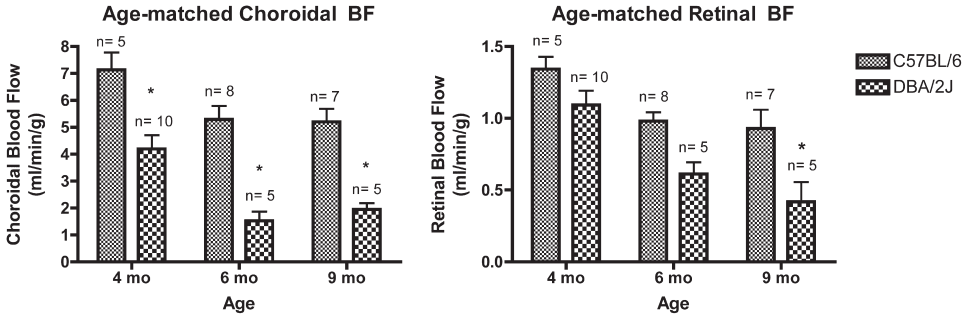

Figure 3. Age-dependent analysis. *Left*: choroidal BF was significantly lower in DBA/2J mice than in C57BL/6 mice at 4 months, 6 months, and 9 months of age. *Right*: retinal BF was significantly lower in DBA/2J mice than in C57BL/6 mice at 9 months of age. $^{*}P < 0.01$, two-way ANOVA.

different at the three time points. Choroidal BF for DBA/2J mice was 4.20 ± 1.6 (range, 2.3–7.1) mL/min/g at 4 months of age, 1.52 ± 0.78 (range, 0.9–2.8) mL/min/g at 6 months of age, and 1.95 ± 0.51 (range, 1.4–2.6) mL/min/g at 9 months of age. Choroidal BF in DBA/2J mice was significantly lower at 6 and 9 months than at 4 months of age. Choroidal BF in DBA/2J mice was significantly lower than in C57BL/6 mice at all age groups ($P < 0.01$ for all age-matched groups). Retinal BF (Fig. 3, right) for C57BL/6 mice was 1.34 ± 0.19 (range, 1.2–1.7) mL/min/g at 4 months of age, 0.98 ± 0.17 (range, 0.7–1.2) mL/min/g at 6 months of age, and 0.93 ± 0.34 (range, 0.3–1.4) mL/min/g at 9 months of age. Although trending downward with age, retinal BF in the C57BL/6 mice was not significantly different at the three time points. Retinal BF for DBA/2J mice was 1.09 ± 0.32 (range, 0.7–1.8) mL/min/g at 4 months of age, 0.61 ± 0.18 (range, 0.4–0.9) mL/min/g at 6 months of age, and 0.42 ± 0.31 (range, 0.1–0.8) mL/min/g at 9 months of age. Retinal BF in DBA/2J mice was significantly lower at 6 and 9 months than at 4 months of age. Retinal BF in DBA/2J mice was significantly lower than in C57BL/6 mice in the 9-month age-matched group ($P < 0.01$).

In addition to age-matched time points, group comparisons were made combining all C57BL/6 and DBA/2J mice (Fig. 4). Choroidal BF for all C57BL/6 mice was 5.43 ± 0.28 (range, 2.5–9.3) mL/min/g versus 2.95 ± 0.45 (range, 0.9–7.1) mL/min/g for the DBA/2J mice ($P < 0.01$). Retinal BF for all C57BL/6 mice was 0.99 ± 0.05 (range, 0.3–1.7) mL/min/g versus 0.80 ± 0.09 (range, 0.1–1.8) mL/min/g for the DBA/2J mice ($P < 0.05$).

Mean arterial pressure of aged C57BL/6 mice was 85 ± 8 (range, 70–99) mm Hg. Mean arterial pressure of aged DBA/2J mice was 80 ± 12 (range, 63–103) mm Hg, which was not significantly different from C57BL/6 mice (Fig. 5).

Discussion

Glaucoma is a complex disease that leads to progressive optic neuropathy with loss of vision or blindness. Increased IOP is a risk factor for glaucoma, and current therapeutic interventions for glaucoma are aimed at lowering IOP.[19] A longstanding hypothesis is that ocular hypertension reduces the ocular perfusion pressure, which causes reduced BF in the ocular circulations, particularly in the prelaminar and laminar optic nerve.[20] IOP-induced deformation of the optic nerve head may also impair axoplasmic transport in the retinal ganglion cell axons, which may damage axons directly or make them more susceptible to ischemic insult.[21]

The DBA/2J mouse model of glaucoma develops ocular hypertension and optic neuropathy with age.[3–6,11,12] The present results indicate that BF in the retinal and choroidal circulations also declines with age in the DBA/2J mouse. Moreover, retinal and choroidal BF in DBA/2J mice is lower than in similarly old control C57BL/6 mice not known to develop optic neuropathy.[22] Given that the murine optic nerve head circulation is derived from the central retinal artery,[23] it seems plausible that BF to the optic nerve may also be reduced and perhaps contributes to the optic neuropathy.

The perfusion pressure gradient driving BF through the ocular circulations is the arterial pressure just outside the eye minus the venous pressure as the veins exit the eye. Venous pressure is slightly greater than IOP or the veins would collapse, and so it is considered approximately equal to the IOP.[24–27] In the older subsets of DBA/2J and C57BL/6 mice tested, there was no significant difference in arterial pressure that would reduce the perfusion pressure and account for the reduced choroidal and retinal BF (Fig. 5). It should be noted that although the iliac arterial pressures in the two mouse strains were similar, the arterial pressure in the mouse central retinal artery supplying the retina and the ciliary arteries supplying the choroid may be lower than the iliac arterial pressure.

In contrast to the similar arterial pressures in the two strains, the IOPs were assumed to be different based on the IOP evaluation by Inman et al.[5] in DBA/2J mice, who found that from 2 to 10 months of age, IOP increased approximately 0.9 mm Hg per month from a starting IOP of approximately 15 mm Hg, with > 80% of 9-month-old DBA/2J mice having IOPs greater than 20 mm Hg. Other investigators have also reported age-dependent IOP increases in the DBA/2J model.[3,4] By contrast, IOP decreases slightly with age in the C57BL/6 strain.[28] Given the documented age-dependent ocular hypertension in

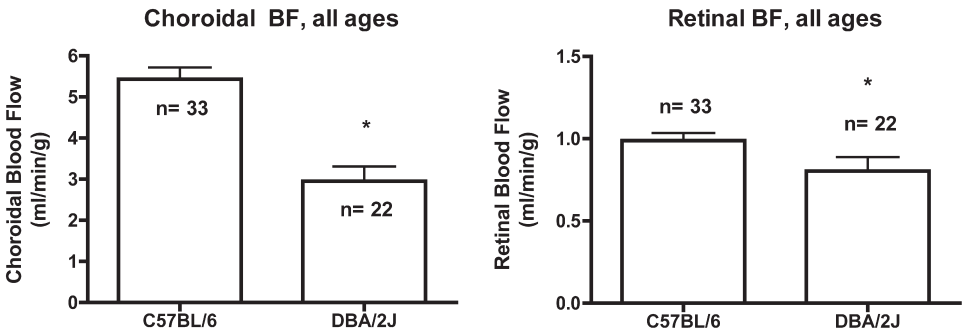

Figure 4. Group analysis. Choroidal (*left*) and retinal (*right*) BFs were significantly lower in DBA/2J mice than in C57BL/6 mice. $^{*}P < 0.05$, unpaired *t*-test.

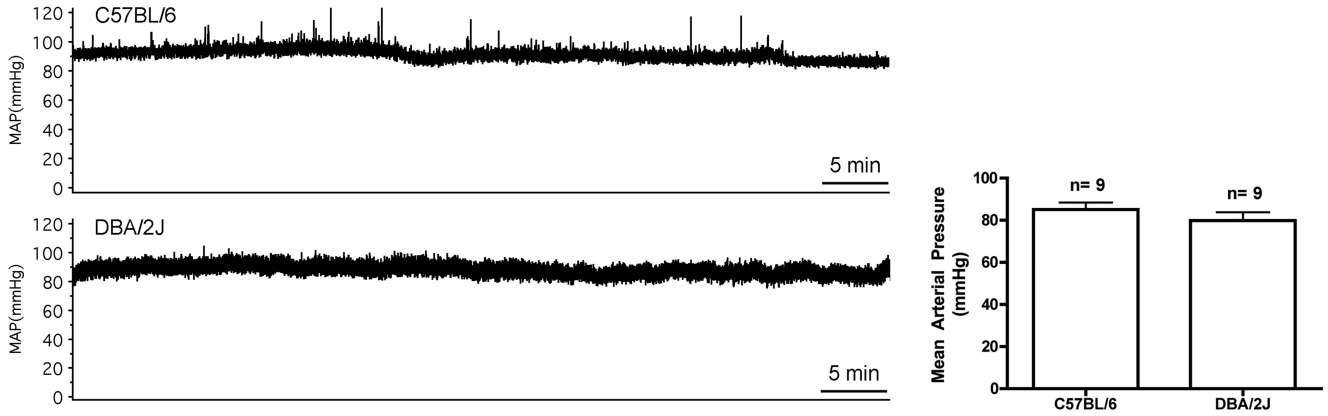

FIGURE 5. Arterial pressure in C57BL/6 and DBA/2J mice. *Left*: hour-long traces of iliac arterial pressure were stable over the duration of a typical MRI study (≈1 hour) with isoflurane administered at 1.6%. *Right*: mean arterial pressure in old C57 mice was not different from that in old DBA mice. $P > 0.05$, unpaired *t*-test.

the DBA/2J strain and normotension in the C57BL/6 strain, it seems likely that reduced perfusion pressure contributed to the lower retinal and choroidal BF in the older DBA/2J mice.

DBA/2J mice also exhibited age-related decline in the scotopic electroretinogram a- and b-wave amplitudes reported in this strain by Bayer et al.[22] It is interesting that those authors found the a-wave declined earlier than the b-wave, which is consistent with insufficient perfusion of the outer retina and with the reduced BF seen earlier in the choroid than in the retina in this study. Also suggestive of BF involvement are the age-dependent decreases and increases in pattern electroretinogram responses to acute increases and decreases in IOP induced by head-down and head-up tilt.[29,30] Depending on the autoregulatory abilities of the murine retinal and choroidal circulations (i.e., their abilities to maintain BF despite changes in perfusion pressure), such alterations in perfusion pressure would cause directionally similar changes in retinal and choroidal BF possibly sufficient to affect retinal function.

There are three limitations of this study that should be noted. First, BF of the mouse optic nerve was not measured, and thus reduced optic nerve BF can only be inferred. Second, though perfusion pressure likely declined with age in the DBA/2J mice, blood pressure and IOP were not measured simultaneously during MRI. Future experiments could manipulate blood pressure and IOP to vary the perfusion pressure and study retinal and choroidal autoregulation in mice, although this is difficult in the MRI scanner. Third, although the ASL-MRI BF measurement is widely used for brain research and has been cross-validated with more established techniques (e.g., positron emission tomography[31] and iodoantipyrine autoradiography[32]), it has not been validated in the mouse eye because no alternative established technique exists for comparison in mice (e.g., microspheres). Despite these limitations, the finding of decreased retinal and choroidal BF in older DBA/2J mice provides new information about this widely used model of glaucoma.

Acknowledgments

The authors thank Rene C. Renteria for insightful discussions.

References

1. Johnson TV, Tomarev SI. Rodent models of glaucoma. *Brain Res Bull.* 2010;81:349–358.
2. McKinnon SJ, Schlamp CL, Nickells RW. Mouse models of retinal ganglion cell death and glaucoma. *Exp Eye Res.* 2009;88:816–824.
3. John SW, Smith RS, Savinova OV, et al. Essential iris atrophy, pigment dispersion, and glaucoma in DBA/2J mice. *Invest Ophthalmol Vis Sci*. 1998;39:951–962.
4. Libby RT, Anderson MG, Pang IH, et al. Inherited glaucoma in DBA/2J mice: pertinent disease features for studying the neurodegeneration. *Vis Neurosci*. 2005;22:637–648.
5. Inman DM, Sappington RM, Horner PJ, Calkins DJ. Quantitative correlation of optic nerve pathology with ocular pressure and corneal thickness in the DBA/2 mouse model of glaucoma. *Invest Ophthalmol Vis Sci*. 2006;47:986–996.
6. Chang B, Smith RS, Hawes NL, et al. Interacting loci cause severe iris atrophy and glaucoma in DBA/2J mice. *Nat Genet*. 1999;21:405–409.
7. Anderson MG, Smith RS, Hawes NL, et al. Mutations in genes encoding melanosomal proteins cause pigmentary glaucoma in DBA/2J mice. *Nat Genet*. 2002;30:81–85.
8. Williams DS, Detre JA, Leigh JS, Koretsky AP. Magnetic resonance imaging of perfusion using spin inversion of arterial water. *Proc Natl Acad Sci U S A*. 1992;89:212–216.
9. Muir ER, Shen Q, Duong TQ. Cerebral blood flow MRI in mice using the cardiac-spin-labeling technique. *Magn Reson Med*. 2008;60:744–748.
10. Muir ER, Duong TQ. MRI of retinal and choroidal blood flow with laminar resolution. *NMR Biomed.* 2011;24:216–223.
11. Schlamp CL, Li Y, Dietz JA, Janssen KT, Nickells RW. Progressive ganglion cell loss and optic nerve degeneration in DBA/2J mice is variable and asymmetric. *BMC Neurosci*. 2006;7:66.
12. Calkins DJ, Horner PJ, Roberts R, Gradianu M, Berkowitz BA. Manganese-enhanced MRI of the DBA/2J mouse model of hereditary glaucoma. *Invest Ophthalmol Vis Sci*. 2008;49:5083–5088.
13. Cheng H, Nair G, Walker TA, et al. Structural and functional MRI reveals multiple retinal layers. *Proc Natl Acad Sci U S A*. 2006;103:17525–17530.
14. Duong TQ, Pardue MT, Thule PM, et al. Layer-specific anatomical, physiological and functional MRI of the retina. *NMR Biomed*. 2008;21:978–996.
15. Duong TQ, Silva AC, Lee SP, Kim SG. Functional MRI of calcium-dependent synaptic activity: cross correlation with CBF and BOLD measurements. *Magn Reson Med*. 2000;43:383–392.
16. Duong TQ, Muir ER. Magnetic resonance imaging of the retina. *Jpn J Ophthalmol.* 2009;53:352–367.
17. Herscovitch P, Raichle ME. What is the correct value for the brain-blood partition coefficient for water? *J Cereb Blood Flow Metab.* 1985;5:65–69.
18. Nair G, Shen Q, Duong TQ. Relaxation time constants and apparent diffusion coefficients of rat retina at 7 Tesla international. *J Imaging Syst Tech*. 2010;20:126–130.
19. Quigley HA. Glaucoma. *Lancet*. 2011;377:1367–1377.

20. Flammer J, Orgul S, Costa VP, et al. The impact of ocular blood flow in glaucoma. *Prog Retin Eye Res.* 2002;21:359–393.
21. Burgoyne CF, Downs JC, Bellezza AJ, Suh JK, Hart RT. The optic nerve head as a biomechanical structure: a new paradigm for understanding the role of IOP-related stress and strain in the pathophysiology of glaucomatous optic nerve head damage *Prog Retin Eye Res*. 2005;24:39–73.
22. Bayer AU, Neuhardt T, May AC, et al. Retinal morphology and ERG response in the DBA/2NNia mouse model of angle-closure glaucoma. *Invest Ophthalmol Vis Sci*. 2001;42:1258–1265.
23. May CA, Lutjen-Drecoll E. Morphology of the murine optic nerve. *Invest Ophthalmol Vis Sci.* 2002;43:2206–2212.
24. Alm A, Bill A. Ocular circulation. In: Kaufman PL, Alm A. *Adler's Physiology of the Eye*. St. Louis: CV Mosby; 1987:183–203.
25. Moses RA. Hydrodynamic model eye. *Ophthalmologica*. 1963;146:137–142.
26. Kiel JW, van Heuven WAJ. Ocular perfusion pressure and choroidal blood flow in the rabbit. *Invest Ophthalmol Vis Sci*. 1995;36:579–585.
27. Maepea O. Pressures in the anterior ciliary arteries, choroidal veins and choriocapillaris Exp. *Eye Res.* 1992;54:731–736.
28. Savinova OV, Sugiyama F, Martin JE, et al. Intraocular pressure in genetically distinct mice: an update and strain survey. *BMC Genet*. 2001;2:12.
29. Nagaraju M, Saleh M, Porciatti V. IOP-dependent retinal ganglion cell dysfunction in glaucomatous DBA/2J mice. *Invest Ophthalmol Vis Sci*. 2007;48:4573–4579.
30. Porciatti V, Nagaraju M. Head-up tilt lowers IOP and improves RGC dysfunction in glaucomatous DBA/2J mice. *Exp Eye Res*. 2010;90:452–460.
31. Ye FQ, Berman KF, Ellmore T, et al. H(2)(15)O PET validation of steady-state arterial spin tagging cerebral blood flow measurements in humans. *Magn Reson Med.* 2000;44:450–456.
32. Tsekos NV, Zhang F, Merkle H, et al. Quantitative measurements of cerebral blood flow in rats using the FAIR technique: correlation with previous iodoantipyrine autoradiographic studies *Magn Reson Med*. 1998;39:564–573.